Amphiphilic and chiral unsymmetrical perylene dye for solid-state dye-sensitized solar cells

Hurmus REFIKER, Hüriye İCİL[*]

Department of Chemistry, Faculty of Arts and Sciences, Eastern Mediterranean University,
Famagusta, N. Cyprus via Mersin 10, TURKEY
e-mail: huriye.icil@emu.edu.tr

A novel amphiphilic, unsymmetrically substituted N-((2S)-2-aminohexanoic acid)-N′-[(S)-1-phenylethyl]-3,4,9,10-perylenetetracarboxydiimide with 2 different chiral centers was synthesized and characterized. Chiral amphiphilicity, which can be tunable between hydrophilic and hydrophobic parts, is responsible for controlled self-assembly through intermolecular hydrogen bonding (N-H $\cdots$ O). The product showed high thermal stability but partial solubility in common organic solvents. We observed 2 isosbestic points at 533 and 611 nm, confirming the presence of overlapped monomer and excimer emissions in the temperature range of 10-80 °C. Fluorescence quenching in m-cresol was attributed to charge-transfer interactions. Importantly, the excited state of the chiral dye can decay only by fluorescence in the solid state, mainly due to O-H $\cdots$ N hydrogen bonds. Novel red-light-emitting (λ_{em} = 658 nm) chiral perylene dye has a great potential for solid-state lighting technologies.

Key Words: Amphiphilic, hydrogen bonding, controlled self-assembly, two chiral centers, unsymmetrical perylene diimide

Introduction

Perylene tetracarboxylic diimides (PDIs), showing high thermal, chemical, and photostability properties, are known as one of the best n-type organic semiconductors.[1] Due to their inherent $\pi - \pi$ interactions, PDIs are known to form self-organized architectures. It has been recorded that increasing the order of perylene molecules enables an increase in exciton diffusion length and an improvement in charge-carrier mobilities, which improves performances of devices such as OLEDs and solar cells.[2] Thus, PDIs find wide applications in light-emitting diodes and field-effect transistors, mainly as charge-generating and electron-transporting materials in

[*]Corresponding author

electrophotographic photoreceptors, solar cells, and other optoelectronic and photonic devices.[3] As a result, self-assembly of organic molecules both in solution and in the solid state is a vital step in designing bottom-up electronic and optoelectronic devices.[4] Precise control of the morphology and properties is a main challenge in supramolecular self-assembly. As a result, precise modulations of the morphology and properties of PDI self-assembly via noncovalent interactions such as $\pi - \pi$ interactions, van der Waals forces, hydrogen bonding, static electronic interactions, and metal-ligand coordination have attracted much interest in the past decade.[5,6]

Besides the tendency of PDIs to aggregate into n-type semiconducting molecular stacks, in the presence of chiral units helical PDI stacks with preferred handedness would be achieved, which could lead to increased charge-carrier mobilities.[7] In addition, the introduction of amphiphilicity is expected to add one more dimension to the self-assembling of PDIs with different morphologies like micelles, vesicles, planar bilayers, and nanotubes, which are affected by environmental parameters such as the nature of the solvent, the ratios of the good and poor solvents, or temperature.[8] In the literature, there are still few reports on amphiphilic unsymmetrical PDIs and nonracemic chiral amphiphilic unsymmetrical PDIs, perhaps due to the difficulties in the synthesis of amphiphilic PDIs.[6] Sun et al. reported the first 2 nonracemic chiral amphiphilic PDIs with enantiomeric α-amino acids.[7] Xeu et al. then synthesized the first soluble nonracemic chiral perylene tetracarboxylic diimide polymers via acyclic diene metathesis polymerization with the use of optically pure l-α amino acid as the starting material.[9] Among some examples of amphiphilic unsymmetric PDIs, N-decylperylene-3,4:9,10-tetracarboxylic-3,4-ethoxyethoxyethoxypropyl-9,10-imide, synthesized by Yang et al., and 1,7-bis-pyridinoyl perylene diimide amphiphile, reported by Xu et al., are available in the literature.[4,5] Very recently, sugar-based and amphiphilic-based perylene diimide derivative N-(l-hexylheptyl)-N′-((4-amino-phenyl)-α-D-glucopyranoside)-perylene-3,4,9,10-tetracarboxylbisimide was synthesized by Huang et al.[8]

Herein, we report the synthesis of an unsymmetrically substituted amphiphilic perylene diimide with 2 different chiral side centers: N-((2S)-2-aminohexanoic acid)- N′-[(S)-1-phenylethyl]-3,4,9,10-perylenetetracarboxy-diimide. The L-lysine hydrophilic part was intentionally selected due to carboxylic acid moiety, which binds to the TiO$_2$ surface. Considering the structure, the hydrogen bonding, together with the $\pi - \pi$ interaction between the PDI rings and hydrophobic/hydrophilic interactions, is expected to drive the molecule to enable a highly ordered structure with a potential for solid-state dye-sensitized solar cells.

Experimental

Materials

Perylene-3,4,9,10-tetracarboxylic dianhydride, (*S*)-(-)-1-phenylethylamine, potassium hydroxide, phosphoric acid, and isoquinoline were supplied by Aldrich. L-lysine was purchased from Sigma. All organic solvents used were of spectroscopic grade unless otherwise stated.

Measurements

Infrared spectra were obtained with KBr pellets using a Mattson Satellite FT-IR spectrometer. The UV/Vis spectra of solutions were recorded with a Varian Cary 100 spectrometer. The UV/Vis spectra of solid states were measured in thin films, using a PerkinElmer UV/VIS/NIR Lambda 19 spectrometer equipped with solid-state accessories. Optical rotation was measured with a Dr. Kernchen Sucromat digital automatic polarimeter at 589

nm and 20 °C. CD spectra were measured on a JASCO 810 spectropolarimeter. Emission spectra of solutions and solid states were measured in thin films, with a Cary Eclipse spectrophotometer equipped with solid-state accessories. Solid-state emission spectra were recorded in the front-face mode with the sample surface oriented at 35° and 55° with respect to the excitation and emission beams, respectively. The excitation was performed at 485 nm. An elemental analysis was conducted with a Carlo-Erba-1106 CHN analyzer. Thermogravimetric analysis (TGA) thermograms were recorded with an STA 449 Jupiter Simultaneous TG-DSC apparatus from NETZSCH, equipped with Balzers QuadStar 422 software. Samples were heated at 10 K min^{-1} in oxygen. A thermal analysis was recorded using a DSC 820 Mettler Toledo instrument.

Synthesis

N-((2S)-2-aminohexanoic acid)-3,4,9,10-perylenetetracarboxylic-3,4-anhydride-9,10 imide (LPMI) was first synthesized according to the procedure mentioned elsewhere and purified as a key intermediate for the preparation of N-((2S)-2-aminohexanoic acid)- N′-[(S)-1-phenylethyl]-3,4,9,10-perylenetetracarboxydiimide (LPPDI, Figure 1). [10,11] N-((2S)-2-aminohexanoic acid)-3,4,9,10-perylenetetracarboxylic-3,4-anhydride-9,10 imide (LPMI, 0.5 g,
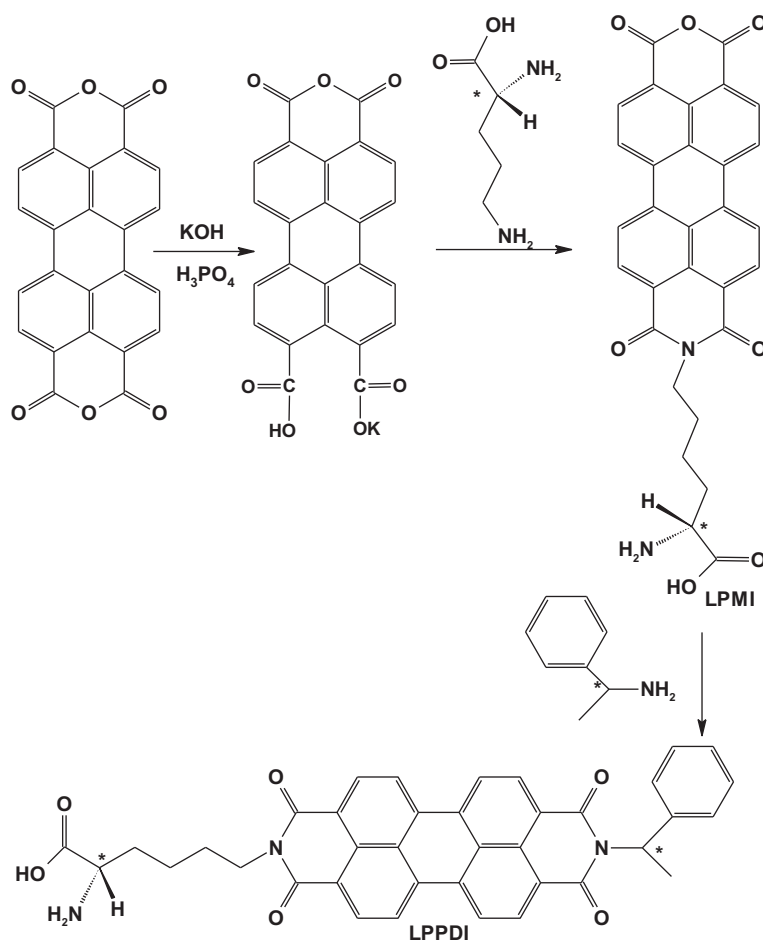
Figure 1. Synthetic routes of LPMI and LPPDI.

0.96 mmol), (*S*)-(-)-1-phenylethylamine (0.366 mL, 2.88 mmol), m-cresol (40 mL), and isoquinoline (4 mL) were then stirred at 80 °C for 1 h under argon atmosphere. The mixture was heated at 100 °C for 2 h, at 120 °C for 2 h, at 160 °C for 3 h, and finally at 200 °C for 4 h. The warm solution was poured into 250 mL of chloroform. The precipitates were collected by vacuum filtration and dried in a vacuum oven at 100 °C. Finally, the crude product was extracted for 48 h with methanol and chloroform in order to remove high-boiling and unreacted reactants using a Soxhlet apparatus, and then dried in vacuum. The structure of the synthesized compound was confirmed by FT-IR, elemental, and thermal analyses. Yield: 85%. $[\alpha]_D^{20}$: -1647.5 (c = 0.02, dimethylformamide [DMF]). FT-IR (KBr, cm^{-1}): ν = 3369 (O-H stretch), 3069 (Ar C-H), 2919, 2853 (aliphatic C-H), 1696 and 1654 (imide C=O), 1593 (Ar C=C stretch), 1577 (N-H bend), 1443, 1407, 1341 (C-N stretch), 1251 (C-O stretch), 1174, 1121, 956 and 852, 811 and 743 (Ar C-H bend). Anal. Calcd. for $C_{39}H_{34}N_3O_6$ (M_w, 640.4): C, 73.11; H, 5.35; N, 6.56. Found: C, 73.29; H, 5.44; N, 6.72. T_d: 415 °C.

Results and discussion

The synthetic route followed, presented in Figure 1 and Table 1, exhibits the solubility properties of LPMI and LPPDI in different solvents at 25 °C. While perylene monoimide (LPMI) is partly soluble only in acetic

Table 1. Solubility of LPMI and LPPDI.

	Solubility^a and color	
	LPMI	LPPDI
Toluene	- -	+ - pale pink
Chloroform	- -	+ - flu. pale orange
TCE	- -	+ - flu. orange
CH$_3$COOH	+ - pale yellow-orange	+ - pale pink
CF$_3$COOH	+ - orange	+ - cherry red
m-Cresol	+ - pink	+ - cherry-red
H$_2$SO$_4$	+ - dark red-blue	+ - dark blue/violet
THF	- -	+ - pale orange
DCM	- -	+ - pale orange
Pyridine	- -	+ - flu. orange
Acetone	- -	+ - pale orange
NMP	- -	+ - brown orange
DMF	+ - pale pink-orange	+ - pale orange
DMAc	- -	+ - flu. pale pink-orange
DMSO	+ - pale pink	+ - pink

Flu.: fluorescent; TCE: 1,1,2,2-tetrachloroethane; DCM: dichloromethane; NMP: N-methylpyrrolidone;

DMF: dimethylformamide; DMAc: dimethylformacetamide; DMSO: dimethyl sulfoxide.

^{a} 0.1 mg in 1.0 mL of solvent at 25 °C. +: soluble; + -: partially soluble (10^{-4}-10^{-7} M); - -: insoluble (after heating/refluxing).

acid, trifluoroacetic acid, m-cresol, sulfuric acid, DMF, and dimethyl sulfoxide (DMSO), the unsymmetrically substituted chiral perylene diimide with 2 chiral centers (LPPDI) has a higher solubility in dipolar aprotic solvents due to the absence of hydrogen bonding interactions. Furthermore, the enhanced solubility could be attributed to the presence of secondary carbon atoms next to nitrogen atoms, forcing the methyl and phenyl substituents out of the plane of the molecule and thereby hampering the face-to-face $\pi-\pi$ stacking of the perylene bisimides.[12] The sterically hindered chiral substituent decreased the short $\pi-\pi$ contacts of the chromophores to a certain extent and therefore increased the solubility.

The IR spectra were fully consistent with the unsymmetrically substituted chiral perylene dye (Figure 2). Figure 2 shows the comparison of LPPDI with its corresponding monoimide, LPMI. Both chiral molecules exhibited strong intermolecular hydrogen bonding, which is characterized by a broad and irregularly shaped band in the region of approximately 3500-1700 cm^{-1}. In the IR spectrum of LPPDI, the characteristic bands of the anhydride carbonyl stretching bands (1766 and 1725 cm^{-1}) disappeared and were replaced by N-imide carbonyl stretching bands (1696 and 1654 cm^{-1}). Similarly, the characteristic band of the C-O-C stretching (1015 cm^{-1}) disappeared and was replaced by a C-N stretching band (1341 cm^{-1}). Additionally, the aliphatic C-O stretching band shifted to 1251 cm^{-1} from 1244 cm^{-1} (LPMI). Other infrared bands of both compounds were very similar (Figure 2).
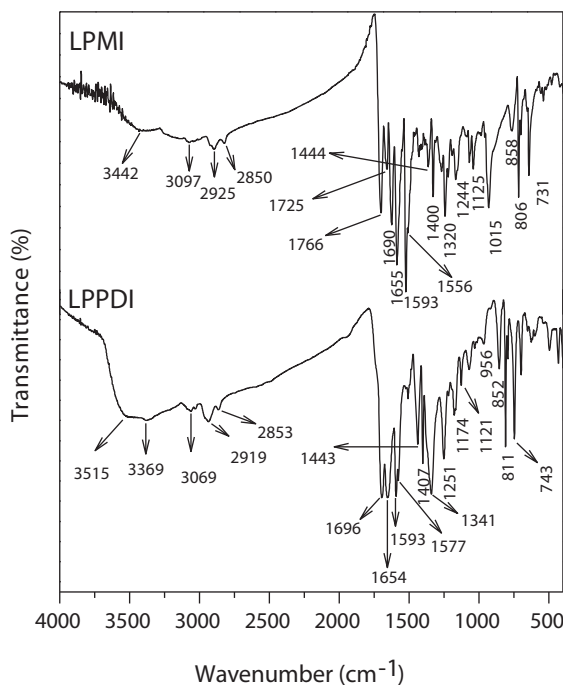
Figure 2. FT-IR spectra of LPMI and LPPDI.

The thermal behavior of LPPDI was investigated by differential scanning calorimetry (DSC; heating rate: 10 K min^{-1}) and TGA (heating rate: 10 K min^{-1}) (Figure 3). The compound did not exhibit any glass transition temperatures in the DSC run. The curve showed a high starting temperature for decomposition (T_d). LPPDI was stable at up to 415 °C. A rapid weight loss of 15.3% of the initial weight occurred between 315 and 425 °C. When the compound was heated to 640 °C, 99.3% of the initial weight was lost rapidly

and a 0.7% char yield was observed. It is noteworthy that LPPDI showed higher thermal stability than the chiral perylene diimide (N,N′-bis((S)-(−)-1-phenylethyl)-3,4,9,10-perylenebis(dicarboximide)), which could be attributed to the strong intermolecular H-bonding interactions.[12]
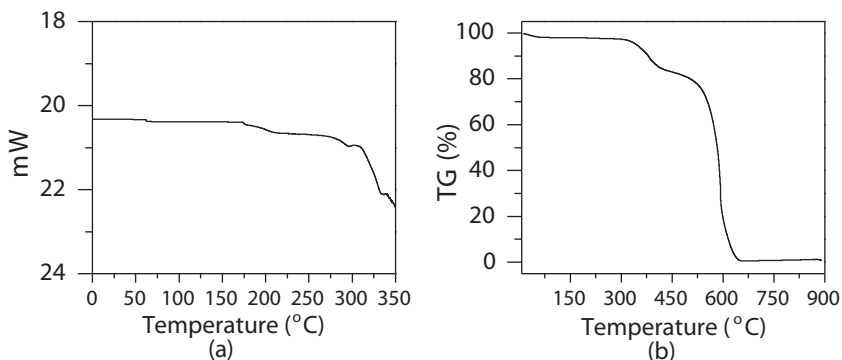
Figure 3. LPPDI: a) DSC thermogram and b) TGA analysis curve, at a heating rate of 10 K min^{-1} under nitrogen and oxygen, respectively.

Self-assembly of the π-conjugated macromolecular systems for formation of a new aggregate structure depends on relative interchromophore orientations and distances that affect UV/Vis absorption spectra.[13] The absorption and emission spectra of unsymmetrically substituted chiral perylene diimide (LPPDI) in nonpolar, polar protic, and dipolar aprotic solvents are represented in Figures 4a-4f ($\lambda_{exc} = 485$ nm). In nonpolar solvents such as chloroform and 1,1,2,2-tetrachloroethane (TCE), LPPDI exhibits 2 characteristic peaks in the range of 450-550 nm and a shoulder at around 456 nm, which respectively correspond to 0-0, 0-1, and 0-2 vibronic transitions.[14] Changes in the absorption ratio between the $0{\rightarrow}0$ and $0{\rightarrow}1$ transitions indicate aggregation, which can be quantified from the absorption ratios where the monomeric PDIs show normal Franck-Condon progression with an $A^{0{\rightarrow}0}/A^{0{\rightarrow}1}$ ratio of approximately 1.6. However, the aggregated PDIs exhibit an inverted intensity distribution among their vibronic states with $A^{0{\rightarrow}0}/A^{0{\rightarrow}1} \leq 0.7$.[15] As depicted in Table 2, the $A^{0{\rightarrow}0}/A^{0{\rightarrow}1}$ ratios for chloroform and TCE are 1.24 and 1.20, respectively, which shows that it is weakly aggregated in these solvents. In another nonpolar solvent, toluene, LPPDI exhibited 2 slightly blue-shifted peaks (3-7 nm) at 524 and 488, and a shoulder at 456 nm, which correspond to 0-0, 0-1, and 0-2 electronic transitions, respectively. In addition, a new unstructured band, centered at around 620 nm, was observed. This new band was attributed to the aggregation effects. As shown in Table 2, a ratio of $A^{0{\rightarrow}0}/A^{0{\rightarrow}1}$ of 1.24 was achieved, which also showed that LPPDI was slightly aggregated in toluene. In the emission spectra of LPPDI in nonpolar solvents, there existed 3 characteristic mirror-image emission bands (toluene: 535, 577, and 628 nm; chloroform: 536, 577, and 626 nm; TCE: 542, 582, and 630 nm), corresponding to 0-0, 1-0, and 2-0 electronic transitions, respectively. A small Stokes shift in the range of 1,250,000-909,091 cm^{-1} was observed. It is worth noting that no excimer or excimer-like peaks were observed, which suggests a similar intermolecular interaction of LPPDI in both the ground state and the excited state.

In the case of polar protic solvents such as acetic acid, an $A^{0{\rightarrow}0}/A^{0{\rightarrow}1}$ ratio of 0.97 suggests an intermediate case, showing both aggregated and monomeric molecules. In trifluoroacetic acid, a new band appeared around 376 nm, which was attributed to the electronic $S_0 {\rightarrow} S_2$ transition with a transition dipole moment perpendicular to the long axis of the molecule.[5] The reversal intensity between the 0-0 and 0-1

transitions could be attributed to the exactly face-to-face-stacked dimer of LPPDI. In H_2SO_4, red-shifted peaks at 599 and 544 nm and a red-shifted shoulder at 512 nm were observed due to protonation at the carbonyl centers. New absorption-band positioning at around 376 nm in m-cresol and 406 nm in H_2SO_4 were observed, most probably due to the electronic $S_0 \rightarrow S_2$ transition with a transition dipole moment perpendicular to the long axis of the molecule, just like in the case of trifluoroacetic acid. Normally, an exactly face-to-face-stacked dimer of PDI will give absorption with an intensity of a 0-0 transition, smaller than that of the 0-1 transition. In both of the solvents' spectra, no reversal intensity between the 0-0 and 0-1 transitions was observed. This suggests either a slipped face-to-face-stacked structure for the molecular self-assembly or the existence of a large portion of nonaggregated LPPDI molecules in solution due to the low stability of the molecular self-assembly.[13]
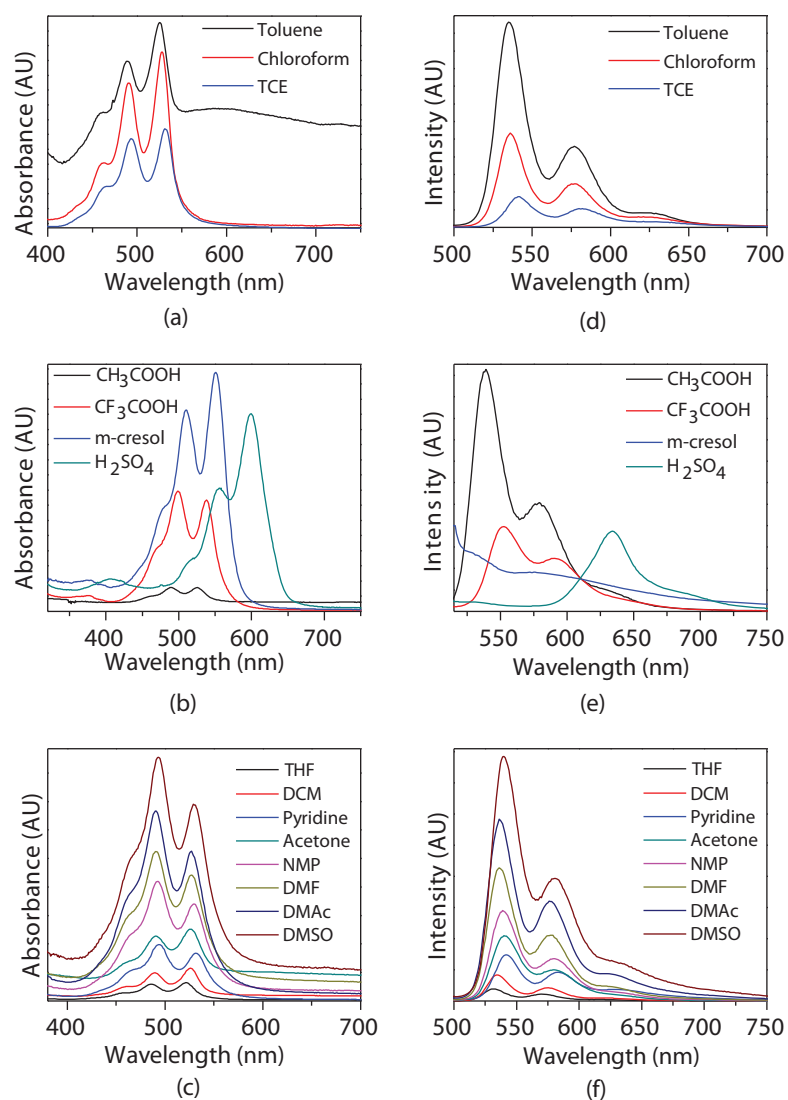
Figure 4. Absorption spectra of LPPDI in a) nonpolar, b) polar protic, and c) dipolar aprotic solvents; and emission spectra of LPPDI in d) nonpolar, e) polar protic, and f) dipolar aprotic solvents; the excitation wavelength of 485 nm.

As seen in Figure 4b, it was clear that in solvents with hydrogen-bonding ability, red-shifted absorption spectra appeared with increasing solvent polarity.

Table 2. Maximum absorption wavelengths $\lambda_{abs\,max}$ (nm), maximum emission wavelengths $\lambda_{eme\,max}$ (nm), Stokes shifts (cm^{-1}), ratios of absorption intensities $A^{0\rightarrow0}/A^{0\rightarrow1}$, and singlet energies Es (kcal mol^{-1}) of LPPDI in different solvents.

Solvents	$\lambda_{abs\,max}$ (nm)	$\lambda_{em\,max}$ (nm)	Stokes shift (cm^{-1})	$A^{0\rightarrow0}/A^{0\rightarrow1}$	E_s ((kcal mol^{-1}))
Toluene	456, 488, *524*, 620	535, 577, 628	909,091	1.24	54.6
Chloroform	459, 491, *528*	536, 577, 626	1,250,000	1.20	54.2
*	470, 508, *555*	658	97087	1.06	51.5
TCE	463, 493, *531*	542, 582, 630	909,091	1.1	53.9
CH$_3$COOH	460, 490, *526*	539, 579, 632	769,231	0.97	54.2
CF$_3$COOH	376, 468, 499, *538*	552, 591, 645	714,286	0.93	51.9
m-Cresol	376, 476, 510, *551*	-	-	1.19	51.7
H$_2$SO$_4$	406, 512, 544, *599*	634, 687	285,714	1.61	47.6
THF	453, 487, *521*	531, 570, 618	1,000,000	1.08	54.9
DCM	455, 490, *527*	534, 575, 623	1,428,571	1.21	54.1
Pyridine	464, 493, *532*	541, 584, 632	1,111,111	0.86	53.6
Acetone	461, 490, *526*	541, 580, 632	666,667	1.11	54.2
NMP	463, 493, *529*	539, 581, 631	1,000,000	0.82	53.9
DMF	461, 490, *527*	536, 577, 629	1,111,111	0.84	54.1
DMAc	461, 490, *527*	536, 577, 629	1,111,111	0.78	54.1
DMSO	464, 493, *530*	540, 581, 633	1,000,000	0.81	53.8

*: in solid state; bolded and italicized wavelengths are absorption wavelengths of 0-0 transitions used for $A^{0\rightarrow0}/A^{0\rightarrow1}$.

Notably, the m-cresol fluorescence of LPPDI was heavily quenched, which could be explained by the photoinduced electron-transfer process from the m-cresol donor to the perylene-acceptor chromophore, due to the formation of an intermolecular O-H...N hydrogen bond between the m-cresol molecule and the NH$_2$ group of LPPDI (Figure 4e). As expected, in the sulfuric acid emission spectrum of LPPDI, a broad red-shifted excimer-like peak was observed at 634 nm, together with a shoulder-like emission at 687 nm. Most probably, the monomeric emission came from the trace of non-face-to-face-stacked LPPDI in the solution, and the excimer's emission was overlapped with the monomeric PDI's emission.[6] A Stokes shift of 285,714 cm^{-1} was achieved, showing that a relatively large amount of nonradiative energy was lost. It is noteworthy that in the CF$_3$COOH and H$_2$SO$_4$ absorption spectra of LPPDI, the intensity of the high-energy vibronic band observed around 376 nm (Figure 4 and Table 2) increased and red-shifted upon the increasing of the solvent polarity and proticity. This could be attributed to the probable protonation interaction of the proton-donor solvent with the amine.

The absorption and emission spectra of LPPDI were also investigated in dipolar aprotic solvents such as tetrahydrofuran (THF), dichloromethane (DCM), pyridine, acetone, N-methylpyrrolidone (NMP), DMF, dimethylacetamide (DMAc), and DMSO (Figure 4). In THF, DCM, and acetone, the ratios of $A^{0\rightarrow0}$ to $A^{0\rightarrow1}$

equaled 1.08, 1.21, and 1.1, respectively, implying the existence of weak aggregation. In the rest of the solvents, such as pyridine, NMP, DMF, DMAc, and DMSO, LPPDI showed 2 absorption peaks, at around 532 and 493 nm, and a shoulder at around 464 nm, which corresponded to vibronic 0-0, 0-1, and 0-2 progressions of the electronic $S_0 \rightarrow S_1$ transition, respectively. In all of those solvents, there was an intensity reversal between the 0-0 and 0-1 transitions, where the ratios of $A^{0\rightarrow0}$ to $A^{0\rightarrow1}$ equaled 0.86, 0.82, 0.84, 0.78, and 0.81 for pyridine, NMP, DMF, DMAc, and DMSO, respectively, suggesting that LPPDI was strongly aggregated and most so in DMAc. In Figure 4c, both red-shifted and blue-shifted absorption peaks can be observed independently of increasing solvent polarity.

Similarly, blue-shifted and red-shifted emissions peaks were observed in the emission spectra of LPPDI in all dipolar aprotic solvents, not correlated with solvent polarity (Figure 4f). A Stokes shift range of 1,428,571-666,667 cm^{-1} was observed, showing the similarity between the ground S_0 and excited S_1 states. Figure 5 shows the temperature-dependent fluorescence spectra of LPPDI in NMP at a concentration of 1 $\times10^{-5}$ M. It can be inferred from Figure 5 that the emission maxima are blue-shifted (1-5 nm) and decreased in emission intensity with increasing temperature from 10 to 80 °C, probably due to the disruption of the intermolecular interactions and π stacking. The blue shift indicated the existence of H-type aggregation upon increasing temperature. At 533 and 611 nm, 2 isosbestic points were observed, which confirmed the existence of overlapped monomer and excimer emissions in the temperature interval from 10 to 80 °C. Furthermore, the presence of the isosbestic points indicated the existence of a closed system consisting of 2 species in equilibrium.[16]
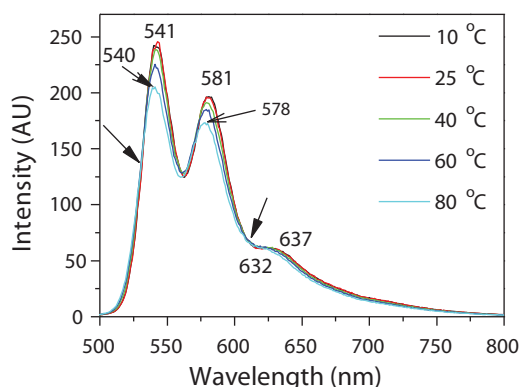
Figure 5. Effect of temperature of emission of LPPDI in NMP at the excitation wavelength of 485 nm.

The absorption and emission spectra of the chiral unsymmetrical perylene in CHCl$_3$ (1 $\times$ 10^{-5} M) and the solid state are shown in Figure 6, and their respective maxima and Stokes shifts ($\Delta\lambda$) are listed in Table 2. The spectra in chloroform nicely obeyed the mirror-image rule and showed a clearly resolved vibronic structure, both in absorption (459, 491, 528 nm) and emission (536, 577, 626 nm), with a small Stokes shift (1,250,000 cm^{-1}). Interestingly, the absorption spectrum of the solid state was very similar to the solution absorption spectrum in terms of spectral shape. Although they became broader and red-shifted, the same 3 clearly resolved absorption bands were observed as in solution for the chiral product (in CHCl$_3$: 459, 491, and 528 nm; in solid state: 470, 508, and 555 nm; Figure 6 and Table 2). The 3 resolved absorption bands were attributed to the presence of weakly interacting π-stacks in the solid state. The large Stokes shift observed for LPPDI in the solid state showed the presence of considerable charge transfer in the excited state (Figure

6). The maximum absorption peak of LPPDI in CHCl$_3$ was observed at 526 nm, and it red-shifted to 555 nm in the solid state, as shown in Figure 6, most likely due to different intermolecular π interactions in the solid state. In addition, the absorption intensities ratios of the 0→0 to 0→1 bands, both in solution and solid states, indicate a weak aggregation tendency, even at a concentration of 1 × 10^{-5} M (Table 2, CHCl$_3$ A$^{0\rightarrow0}$/A$^{0\rightarrow1}$ = 1.23, etc.).[15] In the solid state, LPPDI has a ratio of A$^{0\rightarrow0}$ to A$^{0\rightarrow1}$ of 1.06 (Table 2), which implies an intermediate case, indicating both aggregated as well as monomeric molecules, probably due to intermolecular $\pi - \pi$ stacking and hydrogen bonding interactions.[17−22] Perylene dyes show astonishingly high fluorescence in solution, which is strongly quenched by π stacking in the solid state. Strong fluorescence in the solid state could be achieved with the elimination of this self-quenching.[12] The solid-state emission of LPPDI was taken successfully. The chiral asymmetric perylene dye showed excimer-like emission in red light (λ_{em} = 658 nm, with a full width at half maximum of 66 cm^{-1}), which was very similar to the excimer-like emissions usually observed for weakly interacting π-stacked perylene molecules in solution. Besides these well resolved absorption bands, the excimer-like emission of LPPDI was also thought to be an important indication of weakly interacting π-stacks in the solid state. The rather large red-shifted and excimer-like emission in the solid state indicates that the emitting species are dominantly intermolecular in nature, originating from aggregates and excimers.[23] The solid-state emission spectrum of LPPDI is striking, with a very large Stokes shift (97,087 cm^{-1}) observed, which indicates different intermolecular interactions in both states. It is suggested that excited-state relaxation in the solid state to a lower energy state occurred, whereas larger interperylene interaction took place.[24]
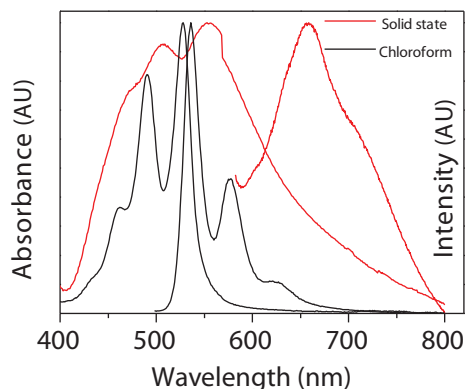
Figure 6. Absorption and emission spectra of LPPDI in the solid state and chloroform at the excitation wavelength of 485 nm.

The emission spectrum of LPPDI was taken at λ_{exc} = 485 nm and the relative fluorescence quantum yields were determined in DMF using N,N′-didodecyl-3,4,9,10-perylenebis(dicarboximide) in chloroform as the standard (N,N′-didodecyl-3,4,9,10-perylenebis(dicarboximide); Φ_f = 1 with respect to rhodamine 101 in ethanol).[25] The lower fluorescence quantum yield of chiral dye (75%) compared to N,N′-bis((S)-(−)-1-phenylethyl)-3,4,9,10-perylenebis(dicarboximide) may be attributed to possible aggregation in solution.

The specific optical rotation ($[\alpha]_D^{20}$, alpha) of LPPDI measured at 20 °C with c = 0.02 mg mL^{-1} in DMF was -1647.5. The high optical activity compared to N,N′-bis((S)-(−)-1-phenylethyl)-3,4,9,10-perylenebis(dicarboximide) is attributed to the asymmetric molecule.[12] The n-π* transitions due to hydrogen bonding inter-

actions are electrically forbidden but magnetically permitted; therefore, in the asymmetric molecule, such a transition can have very low absorption of light but high optical activity. Figure 7 shows the CD spectra of LP-PDI in trifluoroacetic acid. There was a clear, weak positive CD band at 371 nm; however, the remaining bands at 480, 530, and 585 nm were very pallid, probably due to weak intermolecular aggregation and self-assembly. Furthermore, the exciton coupling taking place between perylene and the phenyl $\pi - \pi^*$ transitions gave rise to very pallid signals in the region of 400-550 nm, probably due to the large energy difference between the 2 transitions and/or the unfavorable arrangement between the 2 transition dipoles, which were almost coplanar.[14] In addition, the band observed at 371 nm, which was blue-shifted, compared to the absorption spectrum (375 nm), confirmed a transition dipole moment perpendicular to the long axis of the molecule.
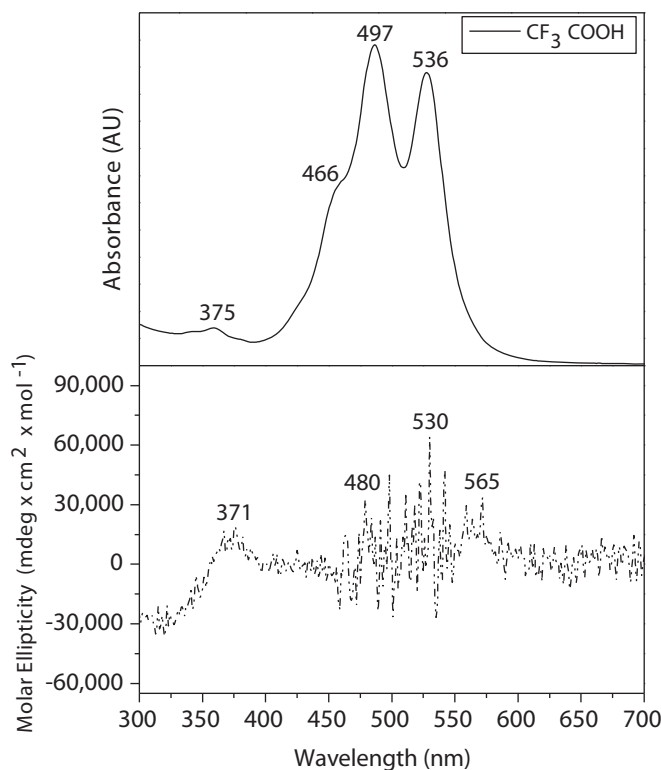
Figure 7. CD spectrum of LPPDI in trifluoroacetic acid (cell = 0.2 cm).

Conclusion

We reported the synthesis of a novel amphiphilic, unsymmetrically substituted N-((2S)-2-aminohexanoic acid)–[(S)-1-phenylethyl]-3,4,9,10-perylenetetracarboxydiimide with 2 chiral centers and with hydrophilic and hydrophobic moieties. Investigation of thermal properties revealed that the chiral dye has very high thermal stability (T_d = 415 °C), which could be attributed to the strong intermolecular H-bonding interactions.

LPPDI exhibited partial solubility in a variety of common organic solvents, possibly due to the intermolecular hydrogen bonding interaction that occurred related to the (Llysine) substituent (N-H $\cdots$ O) with a strongly hydrophilic carboxyl terminal group. Consequently, molar absorption coefficients could not be mea-

sured. At 533 and 611 nm, 2 isosbestic points confirmed the existence of overlapped monomer and excimer emissions in the temperature interval from 10 to 80 $^\circ$C. The H-bonding interactions in polar protic solvents became stronger as acidity increased. Consequently, amphiphilic chiral perylene dye showed a marked red-shift of the absorption and emission bands. Excimer emission in H_2SO_4 at 634 nm (Stokes shift: 285,714 cm^{-1}) resulted in a color change that could be easily recognized. Fluorescence was quenched in m-cresol, possibly due to charge-transfer interactions.

It is noteworthy that the excited state of the chiral dye can decay only by fluorescencing in red light, mainly due to the O-H$\cdots$ N in solid state.[23] Very importantly, the n-orbitals corresponding to lone pairs are strongly stabilized by hydrogen bonds. Thus, the corresponding nπ^* state becomes much higher in energy than the $\pi\pi^*$ state, which results in high fluorescence. It should be noted that weak $\pi-\pi$ stacking and strong O-H$\cdots$N hydrogen bonding interactions were evidently present. Furthermore, chiral amphiphilicity, which can be tunable between hydrophilic and hydrophobic parts, controlled the self-assembly through hydrogen bonding. The novel photonic chiral perylene dye has great potential for solid-state lighting technology, solid-state dye-sensitized solar cells, and photomedicine.

Acknowledgement

References

1. Marcon, R. O.; Brochsztain, S. *J. Phys. Chem. A* **2009**, *113*, 1747-1752.

2. Jancy, B.; Asha, S. K. *Chem. Mater.* **2008**, *20*, 169-181.

3. Sapagovas, V. J.; Gaidelis, V.; Kovalevskij, V.; Undzenas, A. *Dyes Pigments* **2006**, *71*, 178-187.

4. Yang, X.; Xiaohe, X.; Ji, H. F. *J. Phys. Chem. B* **2008**, *112*, 7196-7202.

5. Xu, S.; Sun, J.; Song, G.; Zhang, W.; Zhan, C. *J. Colloid Interf. Sci.* **2010**, *349*, 142-147.

6. Chen, Y.; Kong, Y.; Wang, Y.; Ma, P.; Bao, M.; Li, X. *J. Colloid Interf. Sci.* **2009**, *330*, 421-427.

7. Sun, R.; Xue, C.; Owak, M.; Peetz, R. M.; Jin, S. *Tetrahedron Lett.* **2007**, *48*, 6696-6699.

8. Huang, Y.; Hu, J.; Kuang, W.; Wei, Z.; Faul, C. F. J. *Chem. Commun.* **2011**, *47*, 5554-5556.

9. Xue, C.; Chen, M.; Jin, S. *Poylmer* **2008**, *49*, 5314-5321.

10. Refiker, H. *Symmetrical and Unsymmetrical Perylene Diimide Dyes for Photovoltaic Applications: Chiral, Amphiphilic and Electrochemical Properties*, Eastern Mediterranean University, Famagusta, 2011.

11. Troster, H. *Dyes Pigments* **1983**, *4*, 171-177.

12. Amiralaei, S.; Uzun, D.; Icil, H. *Photochem. Photobiol. Sci.* **2008**, *7*, 936-947.

13. Xue, L.; Wang, Y.; Chen, Y.; Li, X. *J. Colloid Interf. Sci.* **2010**, *350*, 523-529.

14. Pucci, A.; Donati, F.; Nazzi, S.; Barretta, G. U.; Pescitelli, G.; Bari, L. D.; Ruggeri, G. *React. Funct. Polym.* **2010**, *70*, 951-960.

15. Hamilton, T. D. S.; Naqvi, K. R. *Chem. Phys. Lett.* **1968**, *2*, 374-378.

16. Schmidt, C. D.; Bottcher, C.; Hirsch, A. *Eur. J. Org. Chem.* **2009**, *2009*, 5337-5349.

17. Baffreau, J.; Leroy-Lhez, S.; Hudhomme, P.; Groeneveld, M. M.; Van Stokkum, I. H. M.; Williams, R. M. *J. Phys. Chem. A Lett.* **2006**, *110*, 13123-13125.

18. Hippius, C.; Van Stokkum, I. H. M.; Gsanger, M.; Michiel, M.; Groeneveld, M. M.; Williams, M. R.; Wurthner, F. *J. Phys. Chem. C* **2008**, *112*, 2476-2486.

19. Veldman, D.; Chopin, S. M. A.; Meskers, S. C. J.; Groeneveld, M. M.; Williams, R. M.; Janssen, R. A. J. *J. Phys. Chem. A* **2008**, *112*, 5846-5857.

20. Baffreau, J.; Leroy-Lhez, S.; Anh, N. H.; Williams, R. M.; Hudhomme, P. *Chem. Eur. J.* **2008**, *14*, 4974-4992.

21. Williams, M. R. *Turk. J. Chem.* **2009**, *33*, 727-737.

22. Wolffs, M.; Delsuc, N.; Veldman, D.; Anh, V. N.; Williams, M. R.; Meskers, S. C. J.; Janssen, A. J. R.; Huc, I.; Schenning, P. H. I. A. *JACS* **2009**, *131*, 4819-4829.

23. Dreuw, A.; Plotner, J.; Lorenz, L.; Wachtveitl, J.; Djanhan, J. E.; Bruning, J.; Metz, T.; Bolte, M.; Schmidt, M. U. *Angew. Chem. Int. Ed.* **2005**, 44, 7783-7786.

24. Tsumatori, H.; Nakashima, T.; Yuasa, J.; Kawai, T. *Synthetic Met.* **2009**, *158*, 952-954.

25. Icli, S.; Icil, H. *Spectrosc. Lett.* **1996**, *29*, 1253-1257.